



## Hydrodechlorination of tetrachloromethane on alumina- and silica-supported platinum catalysts

Magdalena Bonarowska<sup>a</sup>, Zbigniew Kaszkur<sup>a</sup>, Leszek Kępiński<sup>b</sup>, Zbigniew Karpiński<sup>a,c,\*</sup>

<sup>a</sup> Institute of Physical Chemistry, PAS, ul. Kasprzaka 44/52, PL-01224 Warszawa, Poland

<sup>b</sup> Institute of Low Temperature and Structure Research, PAS, ul. Okólna 2, PL-50422 Wrocław, Poland

<sup>c</sup> Faculty of Mathematics and Natural Sciences-School of Science, Cardinal Stefan Wyszyński University, ul. Wóycickiego 1/3, PL-01938, Warszawa, Poland

### ARTICLE INFO

#### Article history:

Received 19 April 2010

Received in revised form 14 June 2010

Accepted 17 June 2010

Available online 25 June 2010

#### Keywords:

CCl<sub>4</sub> hydrodechlorination

Pt/Al<sub>2</sub>O<sub>3</sub>

Pt/SiO<sub>2</sub>

Effect of metal dispersion

Effect of catalyst regeneration

Metal particle sintering

### ABSTRACT

Two series of alumina- and silica-supported platinum catalysts, representing a wide range of metal dispersion were characterized by CO chemisorption, XRD and TEM, and investigated in the hydrodechlorination of tetrachloromethane at 343–363 K. Catalytic activity of Pt/Al<sub>2</sub>O<sub>3</sub> in CCl<sub>4</sub> hydrodechlorination shows very strong inverse relationship with metal dispersion; highly dispersed Pt samples exhibit very low turnover frequencies. Similar, but much milder trend, was found for silica-supported Pt catalysts. This significant support effect on the catalytic behavior was attributed to an extensive surface chloriding of small Pt particles interacting with Lewis acid sites of γ-alumina. It is suggested that such interactions lead to formation of electrodeficient Pt sites, which are quickly blocked by produced chloride species. On silica, similar in kind metal-support interactions do not occur, and, in effect, deactivation of Pt/SiO<sub>2</sub> catalysts is much less marked. Very strong dependence of catalytic activity of alumina-supported platinum on metal dispersion implies that even very small changes in Pt particle size dispersion during reaction and catalyst regeneration should not be ignored in interpreting variations in the catalytic behavior. Indeed, changes in Pt particle size caused by different regeneration procedures are found to be an important factor in shaping the ultimate hydrodechlorination behavior. Carried out in an oxidative atmosphere for an efficient removal of coke, the regeneration of a highly dispersed Pt/Al<sub>2</sub>O<sub>3</sub> catalyst resulted in a significant growth of metal particles which, in line with the correlation between turnover frequency and metal dispersion established for this catalytic system, exhibited much better performance than that of a freshly reduced catalyst sample. In the case of highly dispersed Pt/SiO<sub>2</sub> catalyst the regeneration also leads to decrease of metal dispersion and corresponding improvement of catalytic activity.

© 2010 Elsevier B.V. All rights reserved.

## 1. Introduction

Catalytic hydrodechlorination (HdCl) of organic wastes containing a variety of toxic and ozone-depleting compounds, such as tetrachloromethane (CCl<sub>4</sub>) is still a subject of great interest. In contrast with the destruction of organic pollutants by incineration, where the value of carbon-containing skeleton is irreversibly lost, HdCl yields valuable hydrocarbons, or other useful and not detrimental chlorine-containing molecules, without formation of waste products [1,2]. In contrast, many of the currently used oxidative methods lead to the formation of dioxins [3], and, obviously, carbon dioxide, contributing to global warming. Recent patent literature shows that search for active and stable catalysts for selective HdCl of CCl<sub>4</sub> to CHCl<sub>3</sub> is still an important chal-

lenge [4,5]. Supported platinum catalysts are particularly useful in selective HdCl of tetrachloromethane to chloroform in the gas phase [6–18].

Two interesting albeit arguable fundamental issues associated with the performance of platinum catalysts concern the problem of the effect of the metal particle size on catalytic behavior in CCl<sub>4</sub> hydrodechlorination and the explanation of the Pt catalyst's behavior after its regeneration. It seems to be a general agreement that very small Pt particles (<1.5 nm) supported on Al<sub>2</sub>O<sub>3</sub> are not useful for HdCl of CCl<sub>4</sub> because they deactivate very quickly with time on stream as a result of irreversible chloriding [9,13,17]. Conversely, larger Pt particles supported on alumina (5–8 nm in size) exhibit very high and stable activity, and outstanding selectivity towards chloroform [9]. In view of those facts, very small (1.9 nm) Pt particles supported on Vycor glass (96% silica) were found, rather unexpectedly, to be exceptionally active and selective in HdCl of CCl<sub>4</sub> [10]. This apparent inconsistency prompted us to perform a more exhaustive search aimed towards establishing a more detailed relation between platinum dispersion and HdCl behavior of alumina- and silica-supported Pt catalysts.

\* Corresponding author at: Institute of Physical Chemistry, Department of Catalysis on Metals, Polish Academy of Sciences, ul. Kasprzaka 44/52, 01-224 Warszawa, Poland. Tel.: +48 223 433 356; fax: +48 226 325 276.

E-mail address: zk@ichf.edu.pl (Z. Karpiński).

**Table 1**

Characteristics of 1.5 wt.% Pt/Al<sub>2</sub>O<sub>3</sub> catalysts. Details of catalyst pretreatment and metal dispersion from CO chemisorption.

Catalyst designation	Catalyst pretreatment: drying/calcalcination, prereduction, sintering (if employed)	CO chemisorption	
		FE <sup>a</sup>	d <sub>Pt</sub> <sup>b</sup> , nm
A1	O <sub>2</sub> , RT/673 K (5 K/min); 673 K, 0.5 h; 10%H <sub>2</sub> /Ar, RT/623 K (1 K/min), 623 K, 2 h	0.691	1.6
A2	4%O <sub>2</sub> /He, RT/573 K (2 K/min), 573 K, 1.5 h; 10%H <sub>2</sub> /Ar, RT/623 K (2 K/min), 623 K, 2 h	0.69	1.6
A3	Air, RT/358 K (5 K/min), 358 K, 0.33 h; 50%H <sub>2</sub> /Ar: RT/673 K (10 K/min), 673, 2 h	0.62	1.8
A4	O <sub>2</sub> , RT/358 K (1 K/min); 358 K, 12 h; H <sub>2</sub> , RT/623 K (10 K/min); 623 K, 2 h	0.595	1.9
A5	4%O <sub>2</sub> + He: RT/443 K; Ar 443 K, 1 h; H <sub>2</sub> , RT/623 K (2 K/min); 623 K, 2 h	0.564	2
A6	As A1 + Ar, RT/773 K (8 K/min); 773 K, 0.5 h	0.361	3.1
A7	Wet A1 (14 days); H <sub>2</sub> , RT/623 K (20 K/min); 623 K, 2 h	0.35	3.2
A8	No calcination; H <sub>2</sub> , RT/473 K (1 K/min); 473 K/673 K (5 K/min), 673 K, 2 h	0.34	3.3
A9	No calcination; H <sub>2</sub> , RT/673 K (5 K/min); 673 K, 2 h	0.13	8.7
A10	No calcination, wet H <sub>2</sub> , RT/673 K (20 K/min); 673 K, 2 h	0.085	13.3

<sup>a</sup> (Platinum) fraction exposed (FE) from CO chemisorption (FE = CO<sub>ad</sub>/Pt<sub>f</sub>).

<sup>b</sup> Pt particle size d<sub>Pt</sub> = 1.13/FE (based on Ref. [22]).

Another controversial issue relates to explanation of large changes in the HdCl behavior of Pt/Al<sub>2</sub>O<sub>3</sub> catalysts brought about by catalyst regeneration [14,18]. Both cited works reported similar effects obtained after catalyst's regeneration using different atmospheres (reductive or oxidative), however offered explanations were different. Based on our finding of an only partial removal of post-reaction coke during regeneration (at 623 K), we suggested [14] that the presence of residual carbonaceous species is beneficial for shaping an extraordinary catalytic performance, creating active centers in the coke structure as recently were proposed in the mechanism of selective hydrogenation of acetylene on Pd catalysts [19,20]. On the other hand, Garetto et al. [18] ascribed similar effect to redispersion of the metallic phase and formation of surface defects. It must be stressed that in both cited works [14,18] the problem of sintering/redispersion of supported Pt phase during HdCl (and regeneration) was not definitely addressed. It seems very important because an increase in Pt particle size caused by regeneration should also be regarded as a possible reason of HdCl activity improvement [21]. Therefore our present effort was to fill this gap, i.e. to inspect possible changes in Pt particle size caused by different regeneration procedures.

## 2. Experimental

### 2.1. Preparation and characterization of the catalysts

Two series of 1.5 wt.% metal-loaded Pt catalysts were prepared by incipient wetness impregnation of alumina (Sasol, 150–200 mesh, 196 m<sup>2</sup>/g) and silica (Davison 62, 120–200 mesh, 268 m<sup>2</sup>/g) with an aqueous solution of chloroplatinic acid, prepared by dissolving Pt wire (Johnson Matthey, Grade 1) in a hot mixture of HCl/HNO<sub>3</sub>, volume ratio 1/10. During impregnation and preliminary drying with infrared lamps, a good mixing was assured by the rotary motion of a beaker containing the catalyst precursor. Then, the solid was further dried overnight in an oven at 358 K. After impregnation and preliminary drying, both catalysts, Pt/SiO<sub>2</sub> and Pt/Al<sub>2</sub>O<sub>3</sub>, were divided into small parts, and by combination of different conditions of calcination (4%O<sub>2</sub>/He or O<sub>2</sub> at 358–673 K), reduction (10%H<sub>2</sub>/Ar or H<sub>2</sub> at 523–673 K) and sintering (in wet H<sub>2</sub> or Ar at 623–803 K) two series catalysts with platinum dispersion in a relatively wide range were obtained.

Metal dispersions (fractions exposed) of the catalysts were assessed from irreversible CO chemisorption at 308 K, using a dual-isotherm method. Prior to chemisorption, the samples were subjected to standard pretreatment described in Section 2.2, and degassed at 673 K for 1.5 h. The static (dual-isotherm) measurements were performed in a fully automated Micromeritics ASAP 2020 instrument using ASAP 2020C V 1.07 software. The basic characteristics of Pt/Al<sub>2</sub>O<sub>3</sub> and Pt/SiO<sub>2</sub> catalysts along with some preparation details are shown in Tables 1 and 2.

XRD experiments were performed on a Rigaku-Denki diffractometer using Ni-filtered Cu K $\alpha$  radiation. Reduced and post-reaction catalyst samples were scanned by a step-by-step technique, at 2 $\theta$  intervals of 0.02°. The high resolution transmission electron microscopy (HRTEM) was recorded with Philips CM20 SuperTwin microscope operating at 200 kV and providing 0.25 nm resolution. Selected Pt/Al<sub>2</sub>O<sub>3</sub> specimens for HRTEM were prepared by dispersing the powder samples in methanol and putting a droplet of the suspension onto a copper microscope grid covered with perforated carbon.

### 2.2. Catalytic tests

The reaction of hydrodechlorination of carbon tetrachloride (provided from a saturator maintained at 273 K) was carried out at atmospheric pressure, in a glass flow reactor. The flows of H<sub>2</sub> and Ar (all 99.999% pure, further purified by passing through MnO/SiO<sub>2</sub> traps), were fixed by using mass flow controllers. Prior to reaction, the catalyst sample was dried at 393 K for 0.5 h in an argon flow and reduced in flowing 10% H<sub>2</sub>/Ar (25 cm<sup>3</sup>/min), ramping the temperature from 393 K to 673 K (at 8 K/min) and kept at 673 K for 3 h. The reaction (at 363 K) was followed by gas chromatography (HP 5890 series II with FID, a 5% Fluorcol/Carbopack B column (10 ft) from Supelco). In all cases the H<sub>2</sub>/CCl<sub>4</sub> ratio of 7 and catalyst weight of ~0.1 g were used. After screening at 363 K and reaching a steady state, the temperature was gradually decreased to 353 K and 343 K, and new experimental points were collected. A typical run lasted ~65 h.

### 2.3. Post-reaction studies of supported Pt catalysts

Post-reaction catalyst samples were investigated by XRD, TEM and temperature programmed hydrogenation (TPH-MS). TPH-MS

**Table 2**

Characteristics of 1.5 wt.% Pt/SiO<sub>2</sub> catalysts. Details of catalyst pretreatment and metal dispersion from CO chemisorption and crystallite size from XRD.

Catalyst designation	Catalyst pretreatment: drying/calcination, prereduction, sintering (if employed)	CO chemisorption		$d_{XRD}^c$ , nm
		FE <sup>a</sup>	$d_{Pt}^b$ , nm	
S1	O <sub>2</sub> , RT/673 K (8 K/min); 673 K, 0.5 h; 10%H <sub>2</sub> /Ar: RT/623 K (2 K/min); 623 K, 2 h	0.893	1.3	<2 <sup>d</sup>
S2	O <sub>2</sub> , RT/673 K (5 K/min), 673 K, 0.5 h; 10%H <sub>2</sub> /Ar: RT/623 K (2 K/min); 623 K, 2 h	0.753	1.5	<2 <sup>d</sup>
S3	As S1 + Ar, RT/773 K (8 K/min), 773, 1 h	0.618	1.8	<2 <sup>d</sup>
S4	4%O <sub>2</sub> /He, RT/403 K (1 K/min); 403 K, 1 h; 10%H <sub>2</sub> /Ar, RT/623 K (1 K/min); 623 K, 2 h	0.393	2.9	3.4 (2.5)
S5	4%O <sub>2</sub> /He, RT/423 K (1 K/min); 423 K, 1 h; 10%H <sub>2</sub> /Ar, RT/623 K (1 K/min); 623 K, 2 h	0.377	3.0	2.7 (2.3)
S6	O <sub>2</sub> , RT/393 K (2 K/min); 393 K, 2 h; H <sub>2</sub> , RT/623 K (5 K/min); 623 K, 2 h	0.332	3.4	3.7 (3.1)
S7	As S1 + Ar, RT/803 K (8 K/min); 803 K, 1 h	0.314	3.6	3.8 (3.1)
S8	As S1 + Ar, RT/803 K (8 K/min); 803 K, 7 h	0.264	4.3	4.3 (3.4)
S9	4%O <sub>2</sub> /He, RT/443 K (1 K/min); 443 K, 1 h; 10%H <sub>2</sub> /Ar, RT/623 K (1 K/min); 623 K, 2 h	0.242	4.7	4.3 (3.4)
S10	No calcination, H <sub>2</sub> , RT/673 K (20 K/min); 673 K, 2 h	0.182	6.2	5.6 (4.3)
S11	No calcination, wet H <sub>2</sub> , RT/673 K (20 K/min); 673 K, 2 h	0.143	7.9	7.4 (5.5)

<sup>a</sup> (Platinum) fraction exposed (FE) from CO chemisorption (FE = CO<sub>ad</sub>/Pt<sub>r</sub>).

<sup>b</sup> Pt particle size  $d_{Pt} = 1.13/\text{FE}$  (based on Ref. [22]).

<sup>c</sup> Pt crystallite size from the 1 1 1 (2 0 0) XRD line broadening using the Scherrer formula.

<sup>d</sup> Invisible XRD reflections from platinum.

runs were performed by flowing a 10% H<sub>2</sub>/He mixture (25 cm<sup>3</sup>/min) at a 10 K/min ramp and followed by mass spectrometry (MA200, Dycor-Ametek, Pittsburgh, USA). Principal attention was paid to *m/z* 15 and 16 (methane evolution), and *m/z* 36 and 38, which are suggestive of HCl liberation from catalysts used.

### 3. Results

Tables 1 and 2 show the basic characteristics of two series of platinum catalysts. Different conditions of catalyst's pretreatment

resulted in the preparation of two series of Pt catalysts, characterized by an extensive range of metal dispersion. The wide range of mean Pt particle sizes ( $d_{Pt}$ ) in reduced catalysts (roughly between 1.5 nm and 10 nm), assessed from metal fraction exposed results, allows to establish the relation between catalytic behavior and metal particle size. Mean crystallite sizes XRD data of reduced Pt/SiO<sub>2</sub> catalysts (Table 2) are in fair agreement with the particle sizes assessed from chemisorption. In the case of Pt/Al<sub>2</sub>O<sub>3</sub> catalysts, a similar consistency was not achieved, most probably because a considerable overlapping of XRD reflections from Pt and  $\gamma$ -alumina forced us to separate a high background ( $\gamma$ -Al<sub>2</sub>O<sub>3</sub>) from relatively

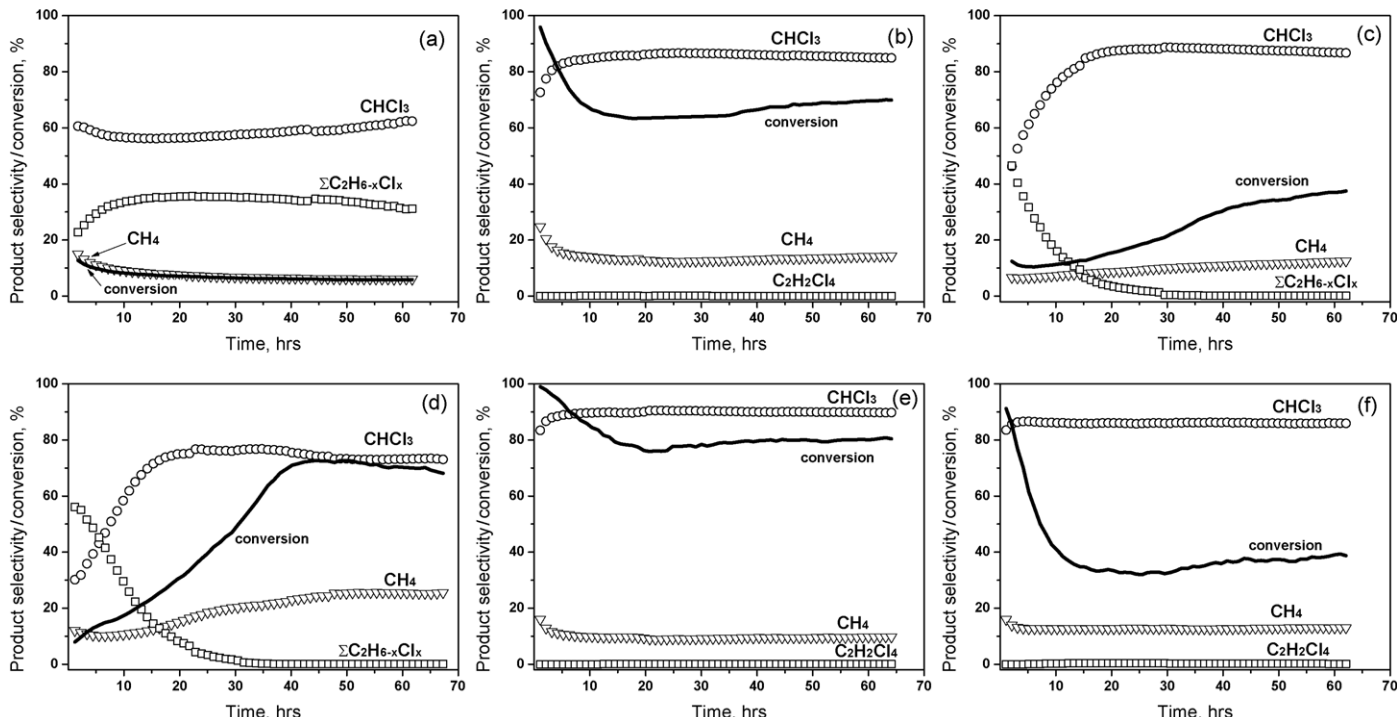


Fig. 1. Time on stream behavior of selected Pt/Al<sub>2</sub>O<sub>3</sub> and Pt/SiO<sub>2</sub> catalysts in CCl<sub>4</sub> hydrodechlorination at 363 K: (a) A3, (b) A6, (c) A9, (d) S2, (e) S8, and (f) S11.

**Table 3**Kinetic data for 1.5 wt.% Pt/Al<sub>2</sub>O<sub>3</sub>: turnover frequencies and selectivities towards CHCl<sub>3</sub> at three reaction temperatures (343, 353 and 363 K) and apparent activation energies.

Catalyst <sup>a</sup> (FE <sup>b</sup> )	TOF <sup>c</sup> , s <sup>-1</sup> ( $S_{CHCl_3}$ , %, at conversion, $\alpha$ , %)			$E_A$ , kJ/mol
	343 K	353 K	363 K	
A1 (0.691)	4.56e-3 (71% at $\alpha$ =3.0%)	5.92e-3 (67.5% at $\alpha$ =3.9%)	8.68e-3 (62% at $\alpha$ =5.7%)	34.4 ± 2.8
A2 (0.69)	3.46e-3 (51% at $\alpha$ =2.1%)	4.48e-3 (46.5% at $\alpha$ =2.8%)	6.94e-3 (37% at $\alpha$ =4.3%)	34.6 ± 8.8
A3 (0.62)	5.60e-3 (70.5% at $\alpha$ =3.2%)	7.19e-3 (64% at $\alpha$ =4.1%)	1.06e-2 (59.5% at $\alpha$ =6.1%)	34.9 ± 5.9
A4 (0.595)	6.61e-3 (55% at $\alpha$ =3.7%)	9.23e-3 (51% at $\alpha$ =5.2%)	1.24e-2 (48% at $\alpha$ =7%)	31.3 ± 1.7
A5 (0.564)	3.95e-3 (66% at $\alpha$ =2.1%)	5.55e-3 (60% at $\alpha$ =3%)	7.81e-3 (54% at $\alpha$ =4.2%)	33.2 ± 0.8
A6 (0.361)	6.47e-2 (77.5% at $\alpha$ =20.9%)	1.64e-1 (83.5% at $\alpha$ =53%)	2.16e-1 (85% at $\alpha$ =69.9%)	61.9 ± 20.4
A7 (0.35)	4.87e-2 (78% at $\alpha$ =16%)	1.15e-1 (84% at $\alpha$ =37.8%)	1.74e-1 (85.5% at $\alpha$ =56.9%)	60.5 ± 15.5
A8 (0.34)	5.22e-2 (81.5% at $\alpha$ =16.7%)	1.12e-1 (85.5% at $\alpha$ =35.8%)	1.60e-1 (87% at $\alpha$ =51.4%)	60.4 ± 10.3
A9 (0.13)	9.72e-2 (81% at $\alpha$ =11.9%)	1.90e-1 (84.5% at $\alpha$ =23.4%)	3.06e-1 (86.5% at $\alpha$ =37.5%)	60.2 ± 4.3
A10 (0.085)	1.27e-1 (82.5% at $\alpha$ =10.8%)	2.60e-1 (85.5% at $\alpha$ =22.1%)	4.06e-1 (87% at $\alpha$ =34.5%)	60.8 ± 7.8

<sup>a</sup> (Platinum) fraction exposed (FE) from CO chemisorption (FE = CO<sub>ad</sub>/Pt<sub>t</sub>).<sup>b</sup> Pt particle size  $d_{Pt} = 1.13/\text{FE}$  (based on Ref. [22]).<sup>c</sup> Based on FE values presented in the first column (values in the brackets) and in Table 1.

broad and not very intense XRD reflections from Pt (results not shown).

Operation at very high reactant conversions, at nearly 100%, easily reachable for HdCl of CCl<sub>4</sub> at reaction temperatures  $\geq 400\text{ K}$  (e.g. [7,8]) is not useful if one searches for structure-sensitivity/insensitivity relations. Therefore our kinetic experiments with HdCl of CCl<sub>4</sub> were intentionally performed at relatively low temperatures, i.e. between 343 K and 363 K. The time-on-stream behavior of HdCl of CCl<sub>4</sub>, including the selectivity to chloroform, methane and chlorinated C<sub>2</sub> products, and catalyst stability for six selected Pt catalysts (of high, medium and low metal dispersions) are shown in Fig. 1. It is seen that in most cases the overall conversion markedly decreased with time on stream, however in two cases (c and d) it increased during reaction run. This behavior, rather unusual for HdCl of CCl<sub>4</sub> on Pt catalysts [9] is accompanied by an increase of CHCl<sub>3</sub> selectivity, associated with a respective decrease of C<sub>2</sub>H<sub>6-x</sub>Cl<sub>x</sub> selectivity. Combination of C<sub>1</sub> into C<sub>2</sub> radicals at an early stage of reaction may result from a relative depletion of surface hydrogen. It was also observed that for a majority of the Pt catalysts the selectivity to CHCl<sub>3</sub> was always lower at the very beginning of the reaction than at steady state. Because this selectivity increase

is accompanied by a corresponding decrease in overall conversion, one concludes that the removal of one chlorine atom from CCl<sub>4</sub> molecule which suffers much less than the total dechlorination route, must be much less demanding reaction than the latter one.

Tables 3 and 4 show the steady state catalytic activities (TOFs), selectivities to CHCl<sub>3</sub> and apparent activation energies. The TOF-metal dispersion relations will be analyzed in Section 4. Used catalysts were characterized by several techniques. The temperature programmed hydrogenation of post-reaction deposits showed a large difference between the state of alumina- and silica-supported highly dispersed Pt catalysts. In contrast to Pt/SiO<sub>2</sub>, non-negligible amounts of chlorine were found in used Pt/Al<sub>2</sub>O<sub>3</sub> catalyst (Fig. 2). Fig. 3 presents the XRD study of reduced and used Pt/SiO<sub>2</sub> catalysts. It is found that the HdCl of CCl<sub>4</sub> does not practically change the XRD profiles of reduced Pt/SiO<sub>2</sub> catalysts. It suggests no change in metal crystallite size during hydrodechlorination for silica-supported Pt catalysts.

Another situation is seen for alumina-supported catalysts. One 1.5 wt.% Pt/Al<sub>2</sub>O<sub>3</sub> catalyst (A2), characterized by a high metal dispersion, was selected for HRTEM studies. Its rather poor catalytic performance was most likely determined by the presence of small

**Table 4**Kinetic data for 1.5 wt.% Pt/SiO<sub>2</sub>: turnover frequencies and selectivities towards CHCl<sub>3</sub> at three reaction temperatures (343, 353 and 363 K) and apparent activation energies.

Catalyst <sup>a</sup> (FE <sup>b</sup> )	TOF <sup>c</sup> , s <sup>-1</sup> ( $S_{CHCl_3}$ , %, at conversion, $\alpha$ , %)			$E_A$ , kJ/mol
	343 K	353 K	363 K	
S1 (0.893)	4.98e-2 (62.5% at $\alpha$ =39.5%)	8.25e-2 (68.5% at $\alpha$ =65.5%)	1.02e-1 (73.5% at $\alpha$ =81.3%)	31.9 ± 6.3
S2 (0.753)	5.30e-2 (65% at $\alpha$ =36.7%)	8.00e-2 (69% at $\alpha$ =55%)	1.00e-1 (73% at $\alpha$ =68.1%)	32.7 ± 4.8
S3 (0.618)	6.93e-2 (72% at $\alpha$ =38.8%)	1.22e-1 (76% at $\alpha$ =68%)	1.49e-1 (80% at $\alpha$ =83.1%)	35.7 ± 8.0
S4 (0.393)	1.12e-1 (71.5% at $\alpha$ =39.5%)	2.08e-1 (76.5% at $\alpha$ =73.4%)	2.45e-1 (78% at $\alpha$ =86.6%)	38.6 ± 10.4
S5 (0.377)	1.12e-1 (64% at $\alpha$ =38%)	1.96e-1 (79% at $\alpha$ =66.2%)	2.56e-1 (80.5% at $\alpha$ =86.8%)	39.6 ± 2.9
S6 (0.332)	1.08e-1 (70.5% at $\alpha$ =32.3%)	1.88e-1 (75.5% at $\alpha$ =56%)	2.37e-1 (78.5% at $\alpha$ =70.4%)	42.6 ± 5.2
S7 (0.314)	1.34e-1 (77.5% at $\alpha$ =36.8%)	2.52e-1 (85% at $\alpha$ =69.5%)	3.24e-1 (86% at $\alpha$ =89.1%)	44.4 ± 9.6
S8 (0.264)	1.25e-1 (81.5% at $\alpha$ =29.7%)	2.57e-1 (88.5% at $\alpha$ =60.9%)	3.40e-1 (90% at $\alpha$ =80.4%)	51.2 ± 9.3
S9 (0.242)	1.23e-1 (75% at $\alpha$ =26.5%)	2.62e-1 (80% at $\alpha$ =56.5%)	3.90e-1 (82% at $\alpha$ =84.2%)	55.6 ± 4.0
S10 (0.182)	8.89e-2 (74% at $\alpha$ =11.5%)	1.91e-1 (82.5% at $\alpha$ =31.2%)	3.31e-1 (85.5% at $\alpha$ =54.1%)	71.1 ± 6.9
S11 (0.143)	8.29e-2 (74% at $\alpha$ =10.6%)	1.82e-1 (82.5% at $\alpha$ =23.4%)	3.02e-1 (86% at $\alpha$ =38.7%)	73.6 ± 8.2

<sup>a</sup> (Platinum) fraction exposed (FE) from CO chemisorption (FE = CO<sub>ad</sub>/Pt<sub>t</sub>).<sup>b</sup> Pt particle size  $d_{Pt} = 1.13/\text{FE}$  (based on Ref. [22]).<sup>c</sup> Based on FE values presented in the first column (values in the brackets) and in Table 2.

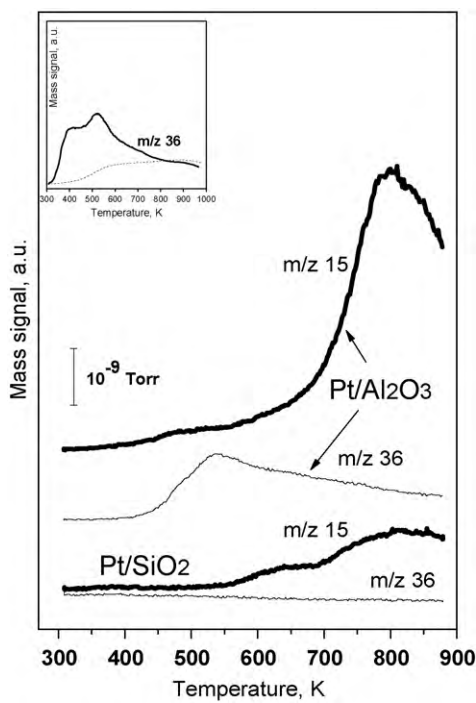


**Fig. 2.** TPH-MS of two Pt catalysts used in hydrodechlorination of  $\text{CCl}_4$ . Pt/ $\text{Al}_2\text{O}_3$ : catalyst A1, Pt/ $\text{SiO}_2$ : catalyst S5. Inset: previous [14] TPH-MS (mass 36) profiles showing HCl evolution from post-reaction 1.5 wt.% Pt/ $\text{Al}_2\text{O}_3$  catalyst (solid line for the freshly reduced catalyst, broken line after regeneration #2).

Pt particles ( $<2$  nm, Table 1). Fig. 4a and b point to a difficult task to identify very small Pt crystallites on  $\gamma\text{-Al}_2\text{O}_3$  by HRTEM, because d spacings (lattice fringes) of Pt are very similar to those of the support. However, both XRD (with some uncertainty mentioned above) and TEM studies of the same catalyst after reaction revealed a definite increase of Pt particles (4 nm from XRD and 5.4 nm from TEM, Fig. 4c–e).

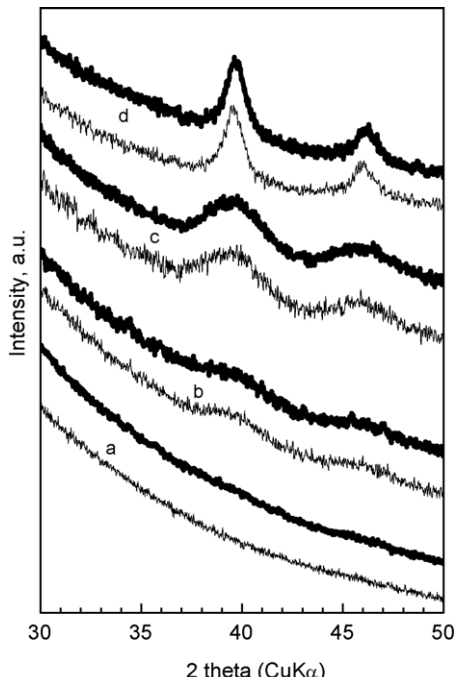


**Fig. 3.** XRD profiles of reduced (thin line) and used (thick line) Pt/ $\text{SiO}_2$  catalysts: (a) S2, (b) S4, (c) S8, and (d) S11.

The first kind of catalyst regeneration after use in hydrodechlorination was realized by hydrogen treatment (10%  $\text{H}_2/\text{Ar}$ , 25  $\text{cm}^3/\text{min}$ ), of spent catalysts carried out at 623 K for 1 h (regeneration #1). The regenerated A2 catalyst was reinvestigated in HdCl of  $\text{CCl}_4$ . The result of catalyst's screening at 363 K is shown in Fig. 5. It is seen that this type of regeneration produces rather moderate changes in the catalytic behavior, especially in overall conversion level, reminding our earlier results (Fig. 4 in Ref. [14]). The second kind of regeneration (regeneration #2) carried out by oxidation at 623 K for 0.5 h in 6%  $\text{O}_2/\text{Ar}$ , 32  $\text{cm}^3/\text{min}$  (and followed by a short rereduction in 10%  $\text{H}_2/\text{Ar}$ , 25  $\text{cm}^3/\text{min}$  at 623 K) led to a much more marked improvement in the catalyst behavior, manifested both in the overall conversion level as well in the selectivity for chloroform (Fig. 6). Again, this effect was earlier discovered by us (Fig. 5 in Ref. [14]). Both regenerated samples of A2 catalyst were investigated by TEM and XRD (Fig. 7). Both methods demonstrated a definite increase of metal particles (compared to the freshly reduced A2 sample): 4 nm from XRD and 5.4 nm from TEM after regeneration #1, and 5 nm from XRD and 6.3 nm from TEM after regeneration #2.

#### 4. Discussion

As mentioned in Section 1, our intention was to determine how the rate and product distribution of  $\text{CCl}_4$  hydrodechlorination catalyzed by platinum catalysts depend on metal particle size of alumina- and silica-supported catalysts. Preparation of two series of differently dispersed Pt catalysts allowed search on the effect of Pt particle size of these catalytic systems. Different catalytic behaviors related to the kind of platinum support will be discussed in some detail. Second part of discussion is the effect and possible explanation of regeneration behavior of Pt/ $\text{Al}_2\text{O}_3$  catalysts.

##### 4.1. Effect of metal dispersion on the HdCl behavior of supported platinum catalysts

Keeping in mind that platinum is an exceptionally good catalytic metal in this reaction and the high price of this precious metal, it appears understandable to carry out research on highly dispersed Pt-based catalysts. However, in contrast to larger Pt particles (5–8 nm in size), very small Pt particles are very prone to excessive chloriding and, in effect, to a drastic deactivation in HdCl of  $\text{CCl}_4$  [9]. Fig. 1 shows that during  $\text{CCl}_4$  hydrodechlorination carried out on both alumina- and silica-supported Pt catalysts characterized by higher metal dispersions (i.e. by smaller Pt particles  $<2$  nm, Tables 1 and 2) large amounts of  $\text{C}_2$ -chlorinated compounds are produced. In the case of alumina-supported catalyst (Fig. 1a) increasing amounts of  $\text{C}_2$  products are accompanied by the decrease of conversion. Such a behavior was also observed by others [8] and explained by coke formation over the Pt/ $\text{Al}_2\text{O}_3$  catalyst. However, in the case of Pt/ $\text{SiO}_2$  catalysts the tendency to  $\text{C}_2$  products ceases after roughly 24 h of time-on-stream (Fig. 1d). At the same time, the overall activity (conversion) is greatly increased. Because no special change in the crystallite size of Pt was found after HdCl (Section 3 and Fig. 3), one must accept that the mentioned effect is associated with different population of various surface species. Large amounts of  $\text{C}_2$  species are suggestive of a relative deficit of surface hydrogen needed for hydrogenative desorption of  $\text{C}_1$  species. It is possible that the active sites on which  $\text{C}_2$  dimers formation occurs are modified to centers which less strongly bind the  $\text{C}_1$  species originating from  $\text{CCl}_4$  molecule.

Apparent activation energy of HdCl of  $\text{CCl}_4$  on platinum catalysts depends on the metal dispersion (Tables 3 and 4). Highly dispersed Pt catalysts, irrespective of the support, exhibit low  $E_A$  level (between 30 kJ/mol and 40 kJ/mol), whereas the low dispersed catalysts show much higher values, 60–70 kJ/mol. Since

more exhausted kinetic studies were not performed in this work and because of a presumable presence of a variety of surface species and side reactions, an ultimate explanation for this difference cannot be offered. At this moment we suggest that the difference in  $E_A$  values follows from different enthalpies of  $\text{CCl}_4$  adsorption: a more negative values of  $\Delta H_{\text{ad}}$  should be characteristic for smaller Pt particles, which on their surface possess a higher fraction of highly unsaturated sites. For  $\text{Pt}/\text{Al}_2\text{O}_3$  catalysts this difference seems to be inversely correlated with the selectivity to  $\text{CHCl}_3$ .

The main result of this report is summarized in Fig. 8, where the relation between metal dispersion and turnover frequency of alumina- and silica-supported Pt catalysts tested in  $\text{HdCl}$  of  $\text{CCl}_4$  at

363 K is presented. It is demonstrated that support selection plays an important role in shaping the catalytic functioning of platinum. The performance of silica-supported Pt catalysts does not depend so much on metal dispersion as do alumina-supported Pt catalysts. Less metal dispersed  $\text{Pt}/\text{SiO}_2$  samples are more active than the highly dispersed ones, but the overall span in TOF is about 3–4, whereas for the  $\text{Pt}/\text{Al}_2\text{O}_3$  system this span approaches nearly two orders of magnitude. Tables 3 and 4 show that the selectivity to chloroform changes less with metal dispersion for  $\text{Pt}/\text{SiO}_2$ . These results are in very good agreement with earlier findings [9,10]. First, the result of Prati and Rossi [10] that very small (1.9 nm) Pt particles supported on Vycor glass (96% silica) are remarkably good for this

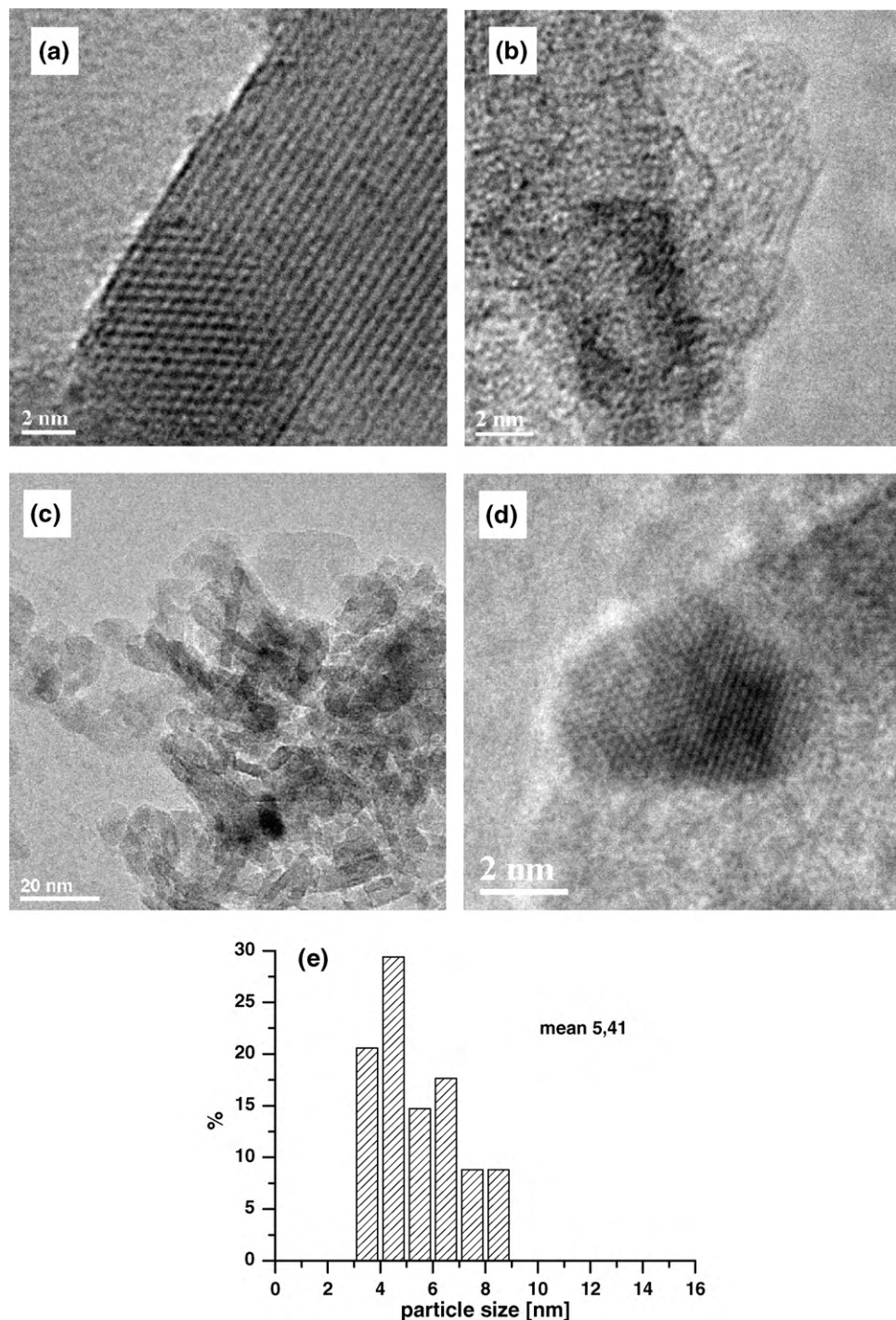


**Fig. 4.** HRTEM micrographs of 1.5 wt.%  $\text{Pt}/\text{Al}_2\text{O}_3$  catalyst (A2) after reduction at 623 K (a and b) and reaction at 363 K (c and d). (e) represents the distribution of metal particle sizes in the  $\text{Pt}/\text{Al}_2\text{O}_3$  catalysts after reaction. In case (a and b) no Pt particles could be detected (see text).

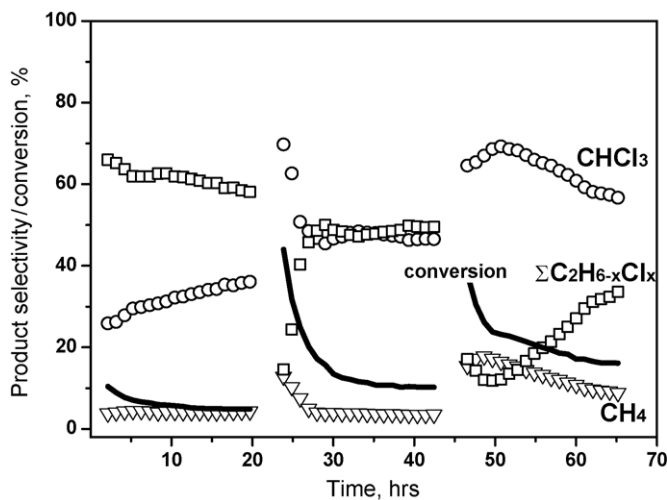


**Fig. 5.** Time on stream behavior of 1.5 wt.% Pt/Al<sub>2</sub>O<sub>3</sub> (A2) catalyst after regeneration #1 (see text).

reaction [10], is supported by the behavior of S3 catalyst, when the selectivity to CHCl<sub>3</sub> was 80%, and the overall activity only twofold lower than the respective values for low dispersed Pt/SiO<sub>2</sub> catalysts (Table 4).

On the other hand, the TOF-FE relation obtained for Pt/Al<sub>2</sub>O<sub>3</sub> catalysts shows an abrupt decrease of TOF in the region of FE between 0.4 and 0.55 (Fig. 8). This result also agrees very well with previous reports [9,21], where very small (<1.5 nm) Pt particles supported on alumina showed severe deactivation and formation of unwanted

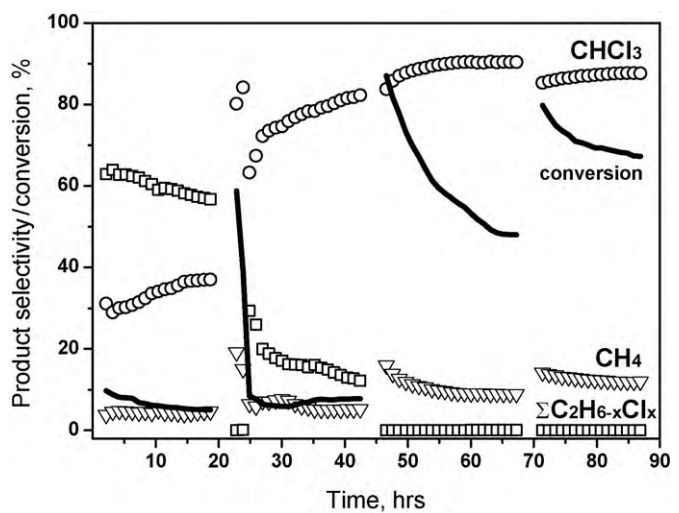


**Fig. 6.** Time on stream behavior of 1.5 wt.% Pt/Al<sub>2</sub>O<sub>3</sub> catalyst (A2) after regeneration #2 (see text).

dimeric products (like C<sub>2</sub>Cl<sub>4</sub> and C<sub>2</sub>Cl<sub>6</sub>). There is evidence that very small Pt particles show electron deficiency established by their inherent character [23] or generated by their interaction with Lewis acid sites in a support (e.g. in  $\gamma$ -alumina) [21,24,25]. The latter reason appears to have a negative effect on the catalytic performance of highly dispersed Pt/Al<sub>2</sub>O<sub>3</sub> samples in HdCl of CCl<sub>4</sub>. Compared to corresponding silica-supported Pt catalysts (for which much weaker metal-support interaction is expected), the highly dispersed Pt/Al<sub>2</sub>O<sub>3</sub> catalysts very quickly deactivate and contain

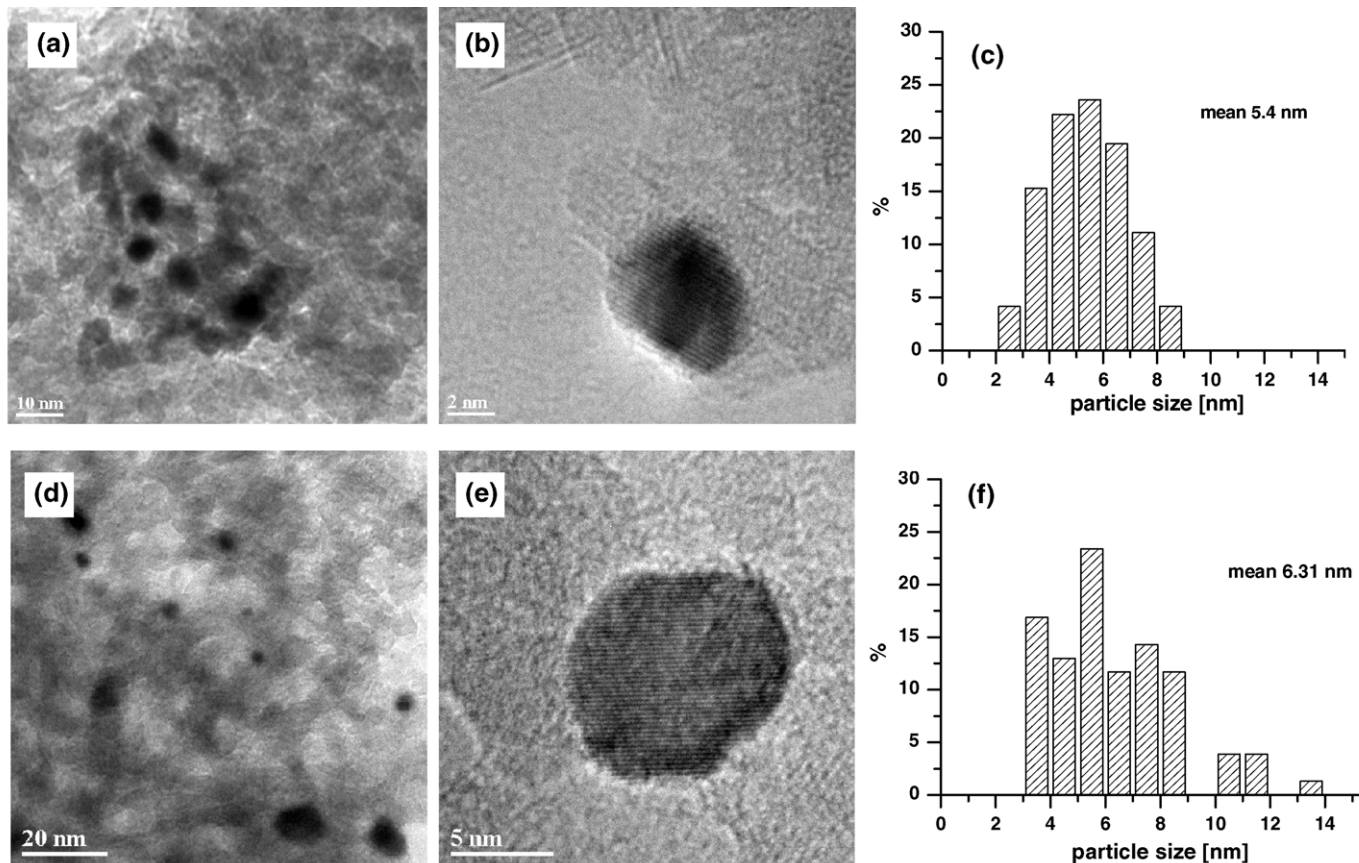


**Fig. 7.** HRTEM micrographs and distributions of metal particle sizes of Pt/Al<sub>2</sub>O<sub>3</sub> catalyst (A2) after type 1 regeneration (a and b) and type 2 regeneration (d and e). (c) and (f) represent respective distributions of metal particle sizes.

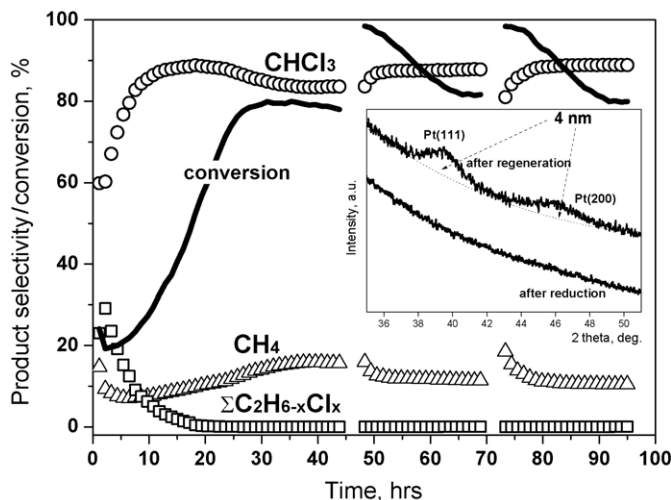


**Fig. 8.** Time on stream behavior of 1.5 wt.% Pt/SiO<sub>2</sub> catalyst (S2) catalyst after regeneration #2 (see text). Inset: XRD profiles of reduced and regenerated samples.

non-negligible amounts of chlorine after reaction (Fig. 2), most probably because of massive liberation of HCl (inherent product of HdCl). On the other hand, larger Pt particles, which should not be characterized by electrodeficiency, show higher catalytic activity and possess much less chlorine after reaction. HCl is known to dissolve Pt compounds, but not the bulk Pt metal [26].

#### 4.2. Regeneration of supported platinum catalysts

Regeneration of deactivated catalysts is very important problem, especially when a reaction is catalyzed by expensive noble metal catalysts. This is actually the case for HdCl of CCl<sub>4</sub> carried out in the presence of alumina-supported Pt catalysts. Both surface chlorine [9,27,28] and carbonaceous residues are regarded as the main reasons of catalyst deactivation [13,16,17,29,30]. Previous reports indicated that regeneration of spent Pt/Al<sub>2</sub>O<sub>3</sub> catalysts carried out in reducing and oxidative atmospheres resulted not only in effective recuperation of deactivated catalysts, but would also bring about a significant improvement of catalytic properties [14,18,31]. Earlier report by Garetto et al. [31] revealed that after regeneration under H<sub>2</sub> the Pt/Al<sub>2</sub>O<sub>3</sub> catalyst exhibited a higher activity and stability. This improved catalytic performance was ascribed [31] to metal redispersion and/or the creation of surface defects, which occurred during the reaction/regeneration cycles in the presence of hydrogen, chlorided compounds and HCl. At about the same time, we reported similar changes caused by regeneration of Pt/Al<sub>2</sub>O<sub>3</sub> catalyst, emphasizing much more effective improvement in the catalytic behavior after regeneration in an air than in hydrogen at 623 K [14]. In their recent paper Garetto et al. [18] do not refer to the results described in [14] but also report much more effective upgrading of a highly dispersed Pt/Al<sub>2</sub>O<sub>3</sub> catalyst when its regeneration is carried out in heated air. The proposed explanation also took into account the metal redispersion and/or the creation of surface defects [18].

Very strong inverse relation between HdCl behavior and metal dispersion of Pt/Al<sub>2</sub>O<sub>3</sub> catalysts established in this work (previous subsection and Fig. 8) implies that it is rather difficult to regard redispersion of highly dispersed Pt catalyst as the basic cause of catalyst amelioration obtained by regeneration. This is because more active and selective (towards CHCl<sub>3</sub>) Pt/Al<sub>2</sub>O<sub>3</sub> catalysts are characterized by lower metal dispersions (Table 3 and Fig. 8). Regeneration of A2 catalyst carried out in this work was performed in similar fashion as our previous experiments [14], but now supplemented by determination of Pt particle sizes after kinetic runs.

Fig. 5 shows the time-on-stream behavior of A2 catalyst subjected to short regeneration in hydrogen at 623 K. It is seen that this type of regeneration slightly increases the overall conversion level, however the selectivity to CHCl<sub>3</sub> is greatly improved. This result (in fair agreement with our previous experiment, Fig. 4 in Ref. [14]) suggests that higher conversion level would be caused by an increase of Pt particles during the reaction/regeneration cycle. This is actually the case because TEM studies of the regenerated catalyst after subsequent reaction run demonstrate a large increase of Pt particles, up to 5.4 nm (4 nm from XRD, Fig. 5). This size increase occurs mainly during the reaction run performed on a freshly reduced catalyst. Fig. 4 shows that during the reaction Pt particles grow also up to 5.4 nm (TEM). The regenerated in hydrogen A2 catalyst has larger Pt particles, however substantial amounts of carbonaceous residues still present on its surface (conclusion from TPH-MS experiment, Fig. 2) do not allow to bring about a level of catalytic activity foreseen by the relation shown in Fig. 8. On the other hand, Fig. 6 shows that the catalyst regenerated in oxidative atmosphere exhibited gradually much better catalytic performance (in fair agreement with our previous results, Fig. 5 in Ref. [18]). Its mean Pt particle size measured by TEM after the reaction was 6.3 nm (5 nm by XRD). The turnover frequency of this catalyst (after considering the adapted FE = 1.13/6.3 = 0.179 [22]) nicely fits the TOF-FE relation for the Pt/Al<sub>2</sub>O<sub>3</sub> catalysts (Fig. 8). It must be said that, for coke removal, regeneration in air is more effective than the regeneration in hydrogen [14], so now we are inclined to consider the growth of Pt particles as the basic reason of catalyst improvement by regeneration procedures.

As it was mentioned earlier, in contrast to highly dispersed alumina-supported samples, used highly dispersed silica-supported Pt catalysts carry only small amounts of Cl species (Fig. 2). Therefore, with exception of highly dispersed Pt/Al<sub>2</sub>O<sub>3</sub> catalysts (which are prone to serious chloriding), carbonaceous residues (coke) should be considered as a basic cause of deactivation of Pt catalysts, in agreement with others [25,26]. Chloride evolution from 1.5 wt.% Pt/Al<sub>2</sub>O<sub>3</sub> catalyst obtained in our previous work (Fig. 1 in Ref. [14]) was included as inset in Fig. 2. It shows that, compared to the used freshly reduced 1.5 wt.% Pt/Al<sub>2</sub>O<sub>3</sub> catalyst, the regenerated (#2) sample of this catalyst contained much smaller amounts of chlorine after reaction. In correspondence with present TEM results, the previously investigated 1.5 wt.% Pt/Al<sub>2</sub>O<sub>3</sub> catalyst (characterized by FE 0.54 after reduction, corresponding to

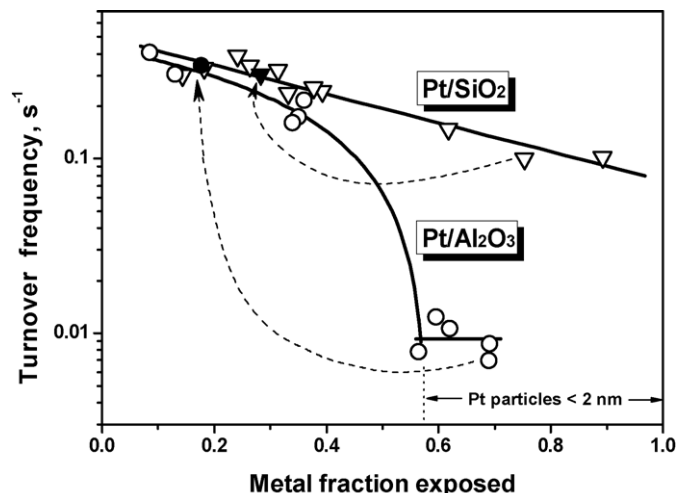


**Fig. 9.** TOF as a function of metal dispersion. Triangles Pt/SiO<sub>2</sub> catalysts, open circles Pt/Al<sub>2</sub>O<sub>3</sub> catalysts. Two black points represent the results obtained for two highly dispersed catalysts subjected to regeneration #2 (circle for A2 catalyst, triangle for S2). The broken arrows symbolize the considerable change in the behavior (both in FE and TOF) caused by regeneration #2.

~2.1 nm particle size) should also exhibit considerable increase of metal particles after regeneration in oxygen.

Regeneration of silica-supported Pt catalysts was not expected to bring about similar changes as in the case of Pt/Al<sub>2</sub>O<sub>3</sub>. Prati and Rossi demonstrated that a series of oxidative regenerations at 623 K of 0.4 wt.% Pt-on-Vycor catalyst resulted in very good reproducibility of the original hydrodechlorination behavior (at steady state, Table 2 in Ref. [10]). In addition, our XRD study (*vide supra*) indicated no change in the crystallite size of Pt after hydrodechlorination (Fig. 3). Application of regeneration #2 to S2 catalyst revealed a similar conversion level as for the same catalyst after reduction (Fig. 8). However, a closer XRD inspection of Pt crystallite size (*d*) showed a 3-fold increase after regeneration (inset in Fig. 8). Such change interpreted as metal dispersion change (according to 1.13/*d*, [22]) satisfactorily fits the FE-TOF relation for Pt/SiO<sub>2</sub> catalysts (Fig. 9). This result confirms the predominant role of metal active phase in catalytic hydrodechlorination on supported metals, while the role of a support is to modify the state of metal by metal-support interactions [1,2,32].

## 5. Conclusions

Catalytic activity of Pt/Al<sub>2</sub>O<sub>3</sub> in CCl<sub>4</sub> hydrodechlorination at 343–363 K shows very strong inverse relationship with platinum dispersion. Very small Pt particles (<2 nm) supported on  $\gamma$ -alumina exhibit low activity and higher selectivity towards C<sub>2</sub>-dimeric species and methane, at the expense of chloroform. Similar, but much less drastic trend, was found for silica-supported Pt catalysts. An extensive chloriding of small Pt particles (presumably electrodeficient due to their interaction with Lewis sites present in  $\gamma$ -alumina) is, apart from surface coking, the basic reason of deactivation of highly dispersed Pt/Al<sub>2</sub>O<sub>3</sub> catalysts. On silica, such strong metal-support interactions do not take place, and, in effect, deactivation of highly dispersed Pt/SiO<sub>2</sub> catalysts is less marked. Changes in Pt particle size caused by different regeneration procedures are found to be an important factor in shaping the hydrodechlorination behavior. Performing regeneration of highly dispersed alumina- and silica-supported Pt catalysts results in a considerable increase of metal particles which, in line with the relation between turnover frequency and metal dispersion established for this catalytic system, exhibit an outstanding performance compared to freshly reduced catalyst samples.

## Acknowledgements

This work was supported by the Polish Ministry of Science and Higher Education within Research Project No. N204 161636. We are

grateful to two reviewers who suggested us perform regeneration of silica-supported Pt catalysts.

## References

- [1] Z. Ainbinder, L.E. Manzer, M.J. Nappa, in: G. Ertl, H. Knözinger, J. Weitkamp (Eds.), *Handbook of Heterogeneous Catalysis*, vol. 4, Wiley-VCH, Weinheim, 1997, p. 1677.
- [2] V.I. Kovalchuk, J.L. d'Itri, *Appl. Catal. A* 271 (2004) 13–25.
- [3] For example, J.R. Hart, *Chemosphere* 54 (2004) 1539–1547.
- [4] L. Cavalli, A. Pasquale, M. Rossi, C. Rubini, US Patent No. 6 627 777 B2 (Date of patent: September 30, 2003), to Süd Chemie MT, S.R.L. (Milan).
- [5] M.T. Holbrook, J.D. Myers, US Patent No. 2007/0225530 A1 (Publication date: 2007-09-27) (to the Dow Chemical Company).
- [6] A.H. Weiss, B.S. Gambhir, R.B. Leon, *J. Catal.* 22 (1971) 245–254.
- [7] H.C. Choi, S.H. Choi, J.S. Lee, K.H. Lee, Y.G. Kim, *J. Catal.* 161 (1996) 790–797.
- [8] H.C. Choi, S.H. Choi, J.S. Lee, K.H. Lee, Y.G. Kim, *J. Catal.* 166 (1997) 284–293.
- [9] Z.C. Zhang, B.C. Beard, *Appl. Catal. A* 174 (1998) 33–39.
- [10] L. Prati, M. Rossi, *Appl. Catal. B* 23 (1999) 135–142.
- [11] J.W. Bae, E.D. Park, J.S. Lee, K.H. Lee, Y.G. Kim, S.H. Yeon, B.H. Sung, *Appl. Catal. A* 217 (2001) 79–89.
- [12] V. Dal Santo, C. Dossi, S. Recchia, P.E. Colavita, G. Vlaic, R. Psaro, *J. Mol. Catal. A* 182–183 (2002) 157–166.
- [13] J.W. Bae, I.G. Kim, J.S. Lee, K.H. Lee, E.J. Jang, *Appl. Catal. A* 240 (2003) 129–142.
- [14] M. Legawiec-Jarzyna, A. Śrębowa, W. Juszczysz, Z. Karpiński, *J. Mol. Catal. A* 224 (2004) 171–177.
- [15] Y.C. Cao, X.Z. Jiang, *J. Mol. Catal. A* 242 (2005) 119–128.
- [16] J.W. Bae, E.J. Jang, B.I. Lee, J.S. Lee, Y.G. Kim, *Ind. Eng. Chem. Res.* 46 (2007) 1721–1730.
- [17] J.W. Bae, J.S. Lee, K.H. Lee, *Appl. Catal. A* 334 (2008) 156–167.
- [18] T.F. Garetto, C.I. Vignatti, A. Borgna, A. Monzón, *Appl. Catal. B* 87 (2009) 211–219.
- [19] A. Borodziński, A. Cybulski, *Appl. Catal. A* 198 (2000) 51–66.
- [20] A. Borodziński, *Catal. Lett.* 71 (2001) 169–175.
- [21] Z.C. Zhang, B.C. Beard, *Appl. Catal. A* 188 (1999) 229–240.
- [22] W. Rachmady, M.A. Vannice, *J. Catal.* 192 (2000) 322–334.
- [23] W.M.H. Sachtler, A.Yu. Stakheev, *Catal. Today* 12 (1992) 283–295.
- [24] S.D. Jackson, J. Willis, G.D. McLellan, G. Webb, M.B.T. Keegan, R.B. Moyes, S. Simpson, P.B. Wells, R. Whyman, *J. Catal.* 139 (1993) 191–206.
- [25] S.D. Jackson, B.M. Glanville, J. Willis, G.D. McLellan, G. Webb, R.B. Moyes, S. Simpson, P.B. Wells, R. Whyman, *J. Catal.* 139 (1993) 207–220.
- [26] D.R. Lide (Editor-in-Chief), *CRC Handbook of Chemistry and Physics 2007–2008*, 88th ed., Taylor & Francis Group, Boca Raton-London-New York, 2008, p. 4–81.
- [27] B. Coq, G. Ferrat, F. Figueras, *J. Catal.* 101 (1986) 434–445.
- [28] M. Martino, R. Rosal, H. Sastre, F.V. Díez, *Appl. Catal. B* 20 (1999) 301–307.
- [29] K.A. Frankel, B.W.-L. Jang, J.J. Spivey, G.W. Roberts, *Appl. Catal. A* 205 (2001) 263–278.
- [30] K.A. Frankel, B.W.-L. Jang, G.W. Roberts, J.J. Spivey, *Appl. Catal. A* 209 (2001) 401–413.
- [31] T.F. Garetto, A. Borgna, J.A. Montoya, D. Acosta, A. Monzón, 13th International Congress on Catalysis, 11–16 July, 2004, Paris, France. Book of Abstracts, vol. 1 and CD ROM. Presentation P6-049.
- [32] A. Morato, C. Alonso, F. Medina, J.L. Garreta, J.E. Sueiras, Y. Cesteros, P. Salagre, D. Tichit, B. Coq, *Catal. Lett.* 77 (2001) 141–145.